IOP Conf. Series: Earth and Environmental Science **163** (2018) 012037 doi:10.1088/1755-1315/163/1/012037

Numerical simulation of unsteady cavitating jet by a compressible bubbly mixture flow method

G Peng[1], **Y Oguma and S Shimizu**
Department of Mechanical Engineering, College of Engineering, Nihon University Tamura-machi, Koriyama, Fukushima 963-8642 Japan

[1] Email: peng@mech.ce.nihon-u.ac.jp

Abstract. Focused on the unsteady behaviour of high-speed water jets with intensive cavitation a numerical analysis is performed by applying a compressible mixture flow method combined with a simplified bubble cavitation model. The mean flow of two-phase mixture is calculated by URANS for compressible flow and the intensity of cavitation in a local field is evaluated by the volume fraction of gas phase varying with the expansion and contraction of bubbles the mean flow field. High-speed submerged water jet issuing from a sheathed nozzle is treated when $\sigma = 0.1$ and $Re = 4.5\times10^5$. The distribution of cavitation clouds predicted approximately agrees with experiment data of visualization observation and the unsteady behaviour of cavitation cloud shedding is captured acceptably. Computational results reveal that cavitation occurs at the entrance of nozzle throat and bubble clouds expand and develop while flowing downstream along the boundary layer. Developed bubble clouds split into small blocks and sheds downstream periodically near the exit of sheath.

1. Introduction

High-speed water jet injected into still water, which is called submerged water jet, has received much attention for its capacity of generating very high cavitation impact pressure in the collapse of cavitation bubbles and widely applied to such as peening of metal materials, decomposition of toxic substances and purification of sewages. Until now, many experimental studies have been made concerning jet driven pressure, shape and size of a nozzle, cavitation number etc. However, the flow structure of cavitating jet and the behaviour of unsteady cavitation clouds are still unclear for the difficulty to observe the interior of cavitating flow [1-3]. For the purpose of performance prediction and optimum design of water jet devices numerical simulation of high-speed water jets with intensive cavitation becomes a task full of challenges [4-6].

In this work, unsteady turbulent cavitating flows caused by high speed submerged water jet are investigated numerically by applying a simplified compressible mixture flow bubble cavitation model. The fluid media of cavitating flows are treated as a two-phase mixture of liquid and gas bubbles dispersing uniformly. The mean flow of two-phase mixture is calculated by the set of Unsteady Reynolds Averaged Navier-Stocks (URANS) equations for compressible flow and the intensity of cavitation is evaluated by the volume fraction of gas bubbles whose radius is estimated with a simplified Rayleigh-Plesset equation. High-speed submerged water jet issuing from a sheathed nozzle is treated and the temporal variation of cavitating flow is investigated. The distribution of cavitation clouds predicted approximately agrees to experiment data of visualization observation and the unsteady behaviour of periodical shedding of cavitation clouds is captured acceptably.

2. Compressible mixture flow bubble cavitation model

The fluid media of cavitating flow are taken as a two-phase mixture of working liquid and cavitation bubbles. The gas bubbles are supposed to disperse in the liquid phase uniformly and its volume faction is denoted as α_G. The liquid volume fraction is written to be α_L. Then, the density of two-phase mixture can be defined as follows by volume averaging.

$$\rho_M = \alpha_L \rho_L + \alpha_G \rho_G \tag{1}$$

where ρ denotes fluid densities and the subscripts L, G, and M respectively do the liquid phase, the gas phase and the two-phase mixture. Then variation of mixture density can be obtained by taking the differential of above equation and it is then arranged to the following form.

$$\frac{1}{\rho_M}\frac{d\rho_M}{dt} = \frac{\alpha_L}{\rho_L}\frac{d\rho_L}{dt} + \frac{\alpha_G}{\rho_G}\frac{d\rho_G}{dt} \tag{2}$$

So, the compressibility of bubble-liquid mixture is be defined as follows.

$$\frac{1}{\rho_M}\frac{d\rho_M}{dt} = \frac{1}{\rho_M c_M^2}\frac{dp_M}{dt} \tag{3}$$

where

$$\frac{1}{\rho_M c_M^2} = \frac{\alpha_L}{\rho_L c_L^2}\frac{\partial p_L}{\partial p_M} + \frac{\alpha_G}{\rho_G c_G^2}\frac{\partial p_G}{\partial p_M} \tag{4}$$

here c denotes the mean sonic speed and p the static pressure. The variations of mixture pressure and the liquid pressure are thought to be equal approximately, namely, for the purpose of simplification.

According to the above equation, we understand that the compressibility of the bubbly mixture depends upon the volume fraction of gas phase as well as the variation of gas pressure, which is determined by bubble size. To determine the compressibility of mixture media both the liquid and the phase are supposed to work exponentially and the following state equations are applied.

$$(p_L + B)/(p_0 + B) = (\rho_L/\rho_{L0})^{n_L} \tag{5}$$

$$p_g/p_{g0} = (\rho_g/\rho_{g0})^{n_g} \tag{6}$$

where the superscript n denote the specific heat ratio and the subscript 0 does a reference state which is taken to be the atmospheric one. B is a constant given to be 3.049×10^8 Pa. The gas phase included in a bubble is assumed to consist of non-condensation gas and vapor which are denoted by subscripted g and v, respectively. Then the sonic speeds in liquid and gas phases are given as follows.

$$\rho_L {c_L}^2 = n_L(p_L + B) \tag{7}$$

$$\rho_G {c_G}^2 = n_g p_g \tag{8}$$

The pressure of non-condensation gas in a bubble is related to the bubble radius R_b. that is to say,

$$p_g = p_0(R_{b0}/R_b)^{3n_L} \tag{9}$$

where, R_{b0} denotes the initial bubble radius at the reference state. Of course, the bubble radius varies rapidly when cavitation occurs corresponding to a sharp decrease of surrounding liquid pressure. It may be solved by the Rayleigh-Plesset equation or similar ones. However, the calculation of these equations is time consuming for the high frequency of bubble oscillation. Thus, the cavitation bubbles are treated as quasi-still one in this work and an estimation of bubble radius is obtained by solving a simplified Rayleigh-Plesset equation approximately [7].

$$\frac{dR_b}{dt} = Sign(\Delta P)\sqrt{\frac{2}{3}\frac{|\Delta P|}{\rho_{L0}}} \tag{10}$$

where $\Delta P = p_g + p_v - p_L$ and $R_b = R_b(\boldsymbol{x}, t)$, which denotes the mean radius of bubbles in a local area $\boldsymbol{x}$ at an arbitrary instant t. Then, the bubble radius may be estimated according the liquid pressure and the sonic speed in the bubbly mixture may be evaluated by equation (4).

Based on the above simplified bubble cavitation model, the flow of bubbly fluid consists of bubbles and surrounding is calculated by using the set of URANS equations for compressible fluid. The variation of temperature caused by cavitation is thought to be very small in the whole flow field and the conservation equation of energy is omitted. Conservation equations of mass and momentum are then closed by introducing the transportation equation of pressure as well as the transport equation of gas volume fraction. The turbulence effect is modeled by adopting the RNG k-ε model for high Reynolds number flow with a modification on the eddy viscosity considering the influence of cavitation.

In an intensively cavitating flow cavitation bubbles may expand greatly and the density of fluid mixture varies sharply in cavitation regions. Thus, the strong compressible bubbly flow region and the weak compressible liquid flow region coexist in a cavitating flow. In order to deal with the great variation of compressibility the set of flow governing equations are solved by using the CIP-CUP (Cubic-Interpolated Propagation/Combined and Unified Procedure) method [8] based on the time splitting technique [7, 9].

3. Computation results and discussions

Figure 1 (a) shows the submerged water jet system to be concerned, where a sheathed orifice nozzle is set up at the bottom of a closed cylindrical chamber full of tap water (deposited one night). Pressured tap water supplied by a plunger pump is injected into the water chamber and a submerged water jet is generated at the given condition. The gauge pressure within the chamber can be adjusted to a given level up to 2.0MPa and the output pressure of the plunger pump can be adjusted within its maximum of 21.0MPa in gauge pressure according to experiment requirements. The throat diameter of the nozzle d = 1.0 mm and the length of nozzle throat is 5.0d. A pipe-like sheath is mounted at the nozzle exit. The inner diameter of the pipe-like sheath is 3.0d and its length is 10.0d. For observing the behaviour of cavitating jet a transparent pressure chamber and a transparent nozzle sheath manufactured by acrylic acid resin were adopted. A high-speed video camera (Phantom Ver7.2) was used to record the

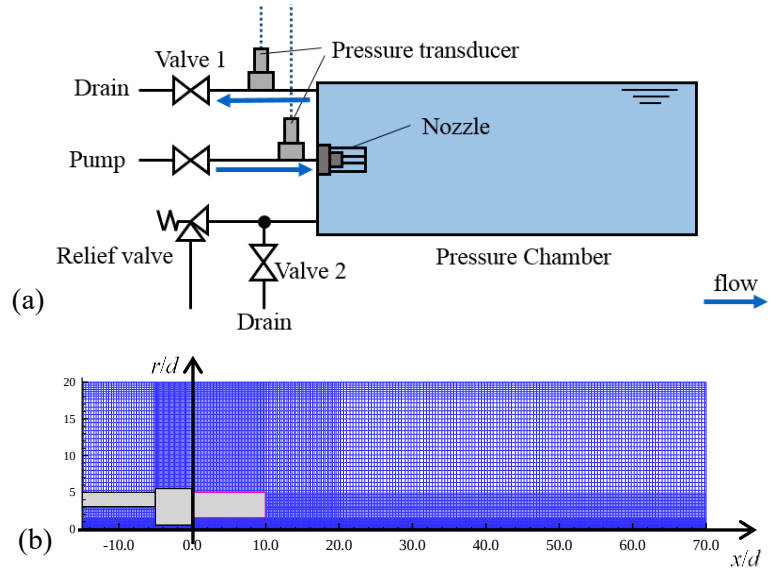

Figure 1. Computation domain for submerged water jet: (a) scheme of water jet system, (b) computation domain and grids.

motion of cavitation clouds and a halogen bulb lamp (Yamazen, HSL 500) was used as light source.

Figure 1 (b) shows the computational domain taken for the numerical simulation of submerged water jet. Focused on the upstream axisymmetric structure the assumption of axisymmetric flow is adopted. The computation domain is taken from 15.0*d* upstream of the nozzle inlet to 70.0*d* downstream of the nozzle exit. The width of computational domain is 25.0*d* in the radial direction. The computation domain is then discretized with quadrilateral structure grid. As for the boundary conditions, a pressure condition is imposed at the inlet according to the given total pressure and the intensity of turbulence was given to be 1.0% of the inflow velocity. At the outlet, a given static pressure is imposed and the Neumann condition was applied to other flow variables such as velocity etc. All the wall boundaries such as the nozzle and the sheath geometries are treated as no-slip walls by applying a universal wall function. As an index for the similarity of cavitation dynamics, the cavitation number σ for the present water jet device is defined as follows.

$$\sigma = \frac{p_o - p_v(T_\infty)}{P_i - p_o} \tag{11}$$

where P_i denotes the injection pressure, p_o the static surrounding pressure at the nozzle exit and p_v the saturated vapor pressure at the reference temperature T_∞. According to the pressure pulsation of the plunger pump employed in the experiments, the jet driven pressure is defined as pulsating one by the following function.

$$P_i = \overline{P}_i\left(1 + c_A \sin(2\pi f t)\right) \tag{12}$$

where $\overline{P}_i$ is the timely averaged pressure. The amplitude coefficient of pressure pulsation is given to be $C_A = 0.25$ and the frequency is given to be $f = 48\,\mathrm{Hz}$.

Figure 2 shows, as an example, the pattern of cavitation cloud shedding in a submerged water jet when the injection pressure $\overline{P}_i = 1.1\,\mathrm{MPa}$ and the discharge pressure p_o = 0.1MPa. The cavitation number σ is calculated to be 0.1 and the Reynolds number Re is about 5.0×10^4 for the concerned case. Figure 2 (a) shows the computational results of developed cavitating jet, where instantaneous distributions of gas volume fraction are demonstrated in a time sequence by contour maps. The areas of high α_G value denoted by red and green colours present axial sections of cavitation cloud and the blue colour indicates the liquid phase. The dark vectors denote the mean velocity in local flow field. It is demonstrated that cavitation clouds expand within the nozzle and the sheath along the shear layer around the core region, and then split into small blocks at the downstream the sheath exit. As shown by the dashed line cavitation clouds denoted by green-like colours stretch out of the sheath and shed downstream periodically. As a comparison, figure 2 (b) shows the experimental results of high-speed video camera visualization observation of developed cavitating jet generated at the same working condition, where the appearance of cavitation jet is demonstrated by a sequence of pictures taken at imaging speed of 27,000 fps. Here, a light source was set at the opposite side of the camera and the pictures were taken under penetrating light condition. Thus, the area full of clear water is observed to be bright one but the area of cavitation cloud including many bubbles is observed to be dark one since the cavitation cloud is almost impermeable to light for the light reflection at bubble surfaces. For the difficulty of observing the interior of the narrow nozzle throat flow visualization observation was focused on the interior of pipe-like sheath, and the shooting area was taken from the nozzle exit (left) to the sheath exit (right). As shown in the figure, cavitation clouds demonstrated by the first picture start to stretch from its minimum length, and then gradually expand to the out of the pipe-like sheath along the shear layer (the 2nd & 3rd pictures) and finally shed downstream as demonstrated by the 4th picture. The dashed line denotes periodical oscillations of cavitation clouds within the sheath.

Comparing figure 2 (a) and (b) we understand that the temporal distributions of gas volume fraction α_G predicted by computation is closed to the experimental results of high-speed camera observation and the periodically shedding of cavitation clouds in water jet is reliably reproduced.

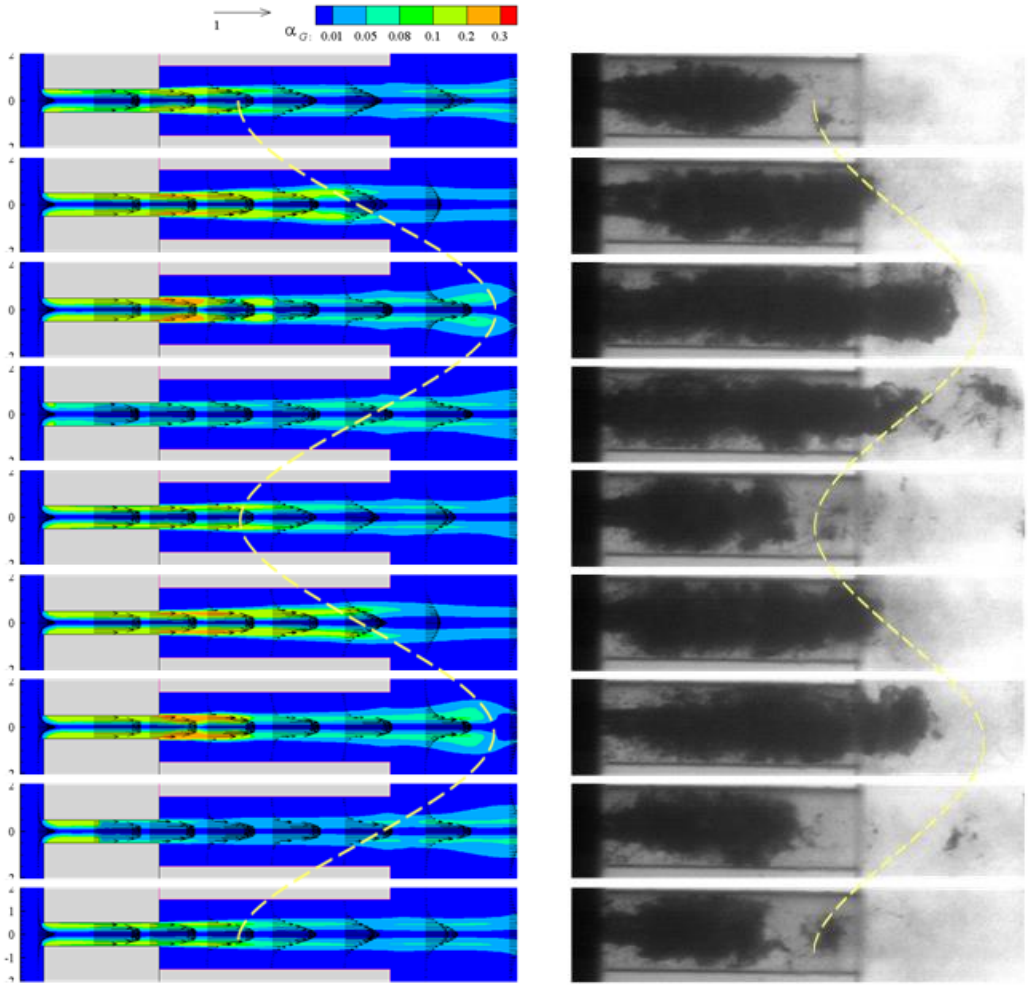

Figure 2. Images of cavitation cloud shedding in time sequence and: (a) Computational result of GVF distributions in time sequence (left) and (b) Sequential images of cavitation clouds recorded via high-speed camera observation (right).

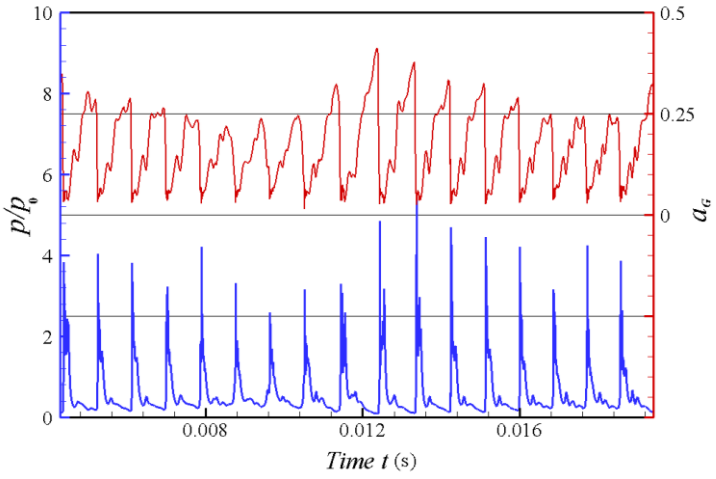

Figure 3. Temporal variations of pressure and GVF at the reference position ($x/d = -4.5$, $r/d = 0.4$) just behind the nozzle throat entrance.

Figure 3 shows, as an example, the computation results of pressure p (absolute) and GVF α_G at the

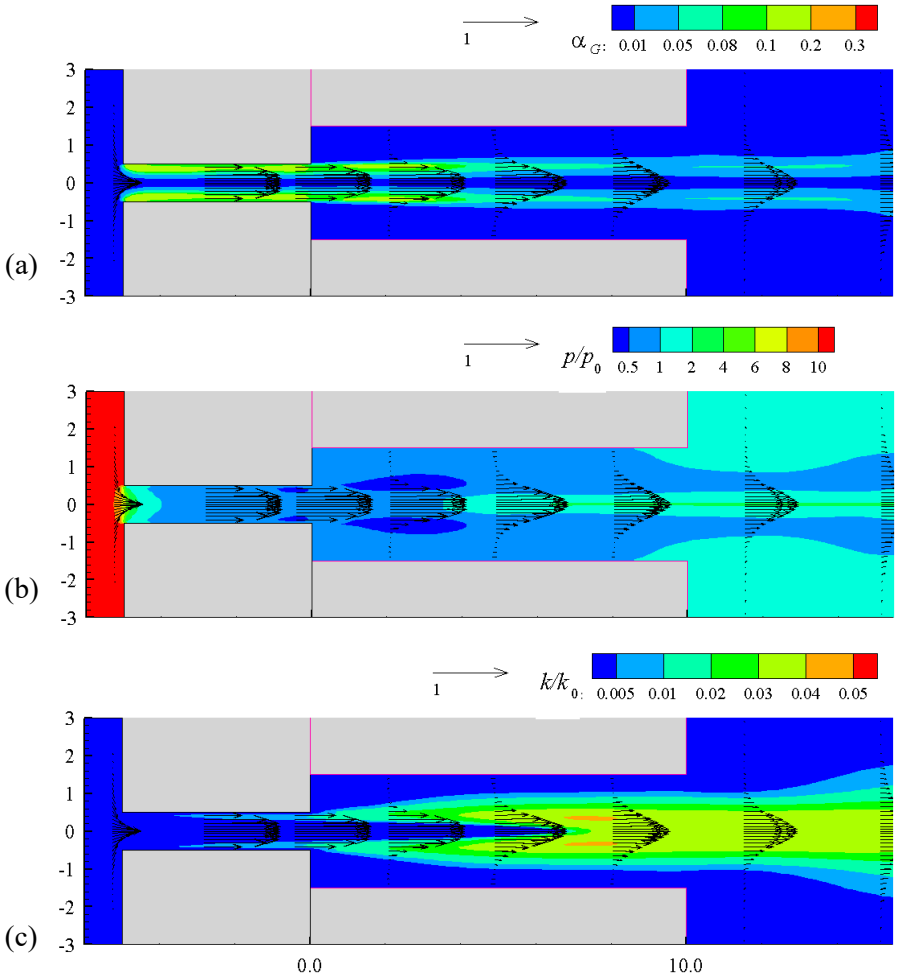

Figure 4. Instantaneous distribution of cavitating water jet: (a) contour map of GVF, (b) contour map of pressure, (c) contour map of turbulence kinetic energy at same moment.

given monitoring position of ($x/d=-4.5$, $r/d=0.45$), which is locates at the entrance of nozzle throat near the wall. The black solid line with solid circles denotes the temporal variation of u_{ref} and the blue dashed line with quadrilaterals does the variation of α_G. It is demonstrated that the flow velocity and the GVF vary periodically almost at the same frequency. FFT (Fast Fourier Transform) analysis reveals that the waveforms fluctuate at two dominant frequencies: $f_1 \approx 55\,\text{Hz}$ and $f_2 \approx 700\,\text{Hz}$. The first dominant frequency, f_1, is close to the frequency of jet driven pressure pulsation, but the second one, f_2, is much higher. It should be related to the bubble clouds expanding and collapsing corresponding to the variation of local flow field [10].

Figure 4 show and instantaneous distribution of cavitating jet, where figure 4 (a), (b) and (c) respectively present the contour map of GVF, the contour map of pressure and the contour map of flow turbulence kinetic energy at the same moment. The vectors demonstrate the velocity variation along the radial direction. According to the figures we know that cavitation occurs near the entrance of nozzle throat and develops along the shear layer within the nozzle and the sheath. The mean flow velocity varies sharply in the radial direction through the shear layer for effect of cavitation bubbles. Thus, the core velocity of cavitating jet decays slowly compared to the case of no-cavitation jet. Figure 4 (b) demonstrates that liquid pressure decreases sharply at the entrance of nozzle. The minimum pressure takes place near the inlet of nozzle sheath and its value reaches to 0.01 MPa in absolute

pressure. Comparing figure 4 (c) and (a) we may understand that the turbulence energy mainly takes place in the shear layer at the downstream behind the nozzle throat, and it indicates a lower value in the boundary layer within the nozzle where cavitation clouds is concentrated.

4. Conclusions

Focused on the unsteady behaviour of intensively cavitating jets, a practical compressible mixture-flow bubble-cavitation model is developed for the simulation of turbulent cavitating flows. The model has been applied to treat the unsteady cavitating flow caused by submerged water jets. The distribution of cavitation clouds predicted approximately agrees with experiment data of visualization observation and the unsteady behaviour of cavitation cloud shedding is captured acceptably.

Computational results demonstrate that: (1) Cavitation occurs at the entrance of nozzle throat and cavitation bubble clouds expand and develop while flowing downstream along the boundary layer. (2) Developed bubble clouds split into small blocks and sheds downstream periodically near the exit of sheath. (3) Flow turbulence mainly takes place in the in the shear layer behind the nozzle throat.

Acknowledgments

This work was partly supported by JSPS, Grant-in-Aid for Scientific Research (C) (No. 17K06169). The authors would like also to thank Mr. T Ito and Miss A Wakui for their assistance in experiments.

References

[1] Kalumuck K M and Chahine G L 2000. The use of cavitating jets to oxidize organic com-pounds in water. *J. Fluids Eng.*, 122, 465-470.
[2] Nishimura S et al. 2012. Similarity law on shedding frequency of cavitation cloud induced by a cavitating Jet, *J. Fluid Sci. & Tech.*, 7(3), 405-420.
[3] Sato K, Taguchi Y and Hayashi S 2013. High speed observation of periodic cavity behavior in a convergent-divergent nozzle for cavitating water jet, J. Flow Control, Measurement & Visualization, 1, 102-107.
[4] Qin Z, Bremhorst K and Alehossein H 2007. Simulation of cavitation bubbles in a convergent–divergent nozzle water jet, J. Fluid Mech., 573, 1-25.
[5] Iga Y and Konno T 2012. Numerical analysis of the influence of acceleration on cavitation instabilities that arise in cascade, Int. J. Fluid Machinery and Systems, 5, 1-9.
[6] Peng G and Shimizu S 2013 Progress in numerical simulation of cavitating water jets, J. Hydrodynamics, 25, 502-509.
[7] Peng G, Yang C, Oguma Y and Shimizu S 2016. Numerical analysis of cavitation cloud shedding in a submerged water, J. Hydrodynamics (B), 28(6), 986-993.
[8] Peng G, Shimizu S and Fujikawa S 2011. Numerical simulation of cavitating water jet by a compressible mixture flow method, J. Fluid Sci. & Tech., 6, 499-509.
[9] Peng G, Ishizuka M and Hayama S, 2001. An improved CIP-CUP method for submerged water jet flow simulation, JSME Int. J. (B): Fluids and Thermal Eng., 44(4), 497-504.
[10] Zhou Y et al. 2016. Fluid-Structure-Sound Interactions and Control, Springer-Verlag, Berlin Heidelberg, 229-234.